2011

Consistent model of magnetism in ferropnictides

Aleksander L. Wysocki
University of Nebraska-Lincoln, awysocki@iastate.edu

Kirill D. Belashchenko
University of Nebraska-Lincoln, belashchenko@unl.edu

Vladimir P. Antropov
Ames Laboratory, US Department of Energy, antropov@ameslab.gov

Follow this and additional works at: http://digitalcommons.unl.edu/physicsbelashchenko

Consistent model of magnetism in ferropnictides

A. L. Wysocki,[1] K. D. Belashchenko,[1] and V. P. Antropov[2]

[1]*Department of Physics and Astronomy and Nebraska Center for Materials and Nanoscience,*
University of Nebraska-Lincoln, Lincoln, Nebraska 68588, USA
[2]*Ames Laboratory, Ames, Iowa, 50011, USA*
(Dated: September 25, 2013)

Abstract

The discovery of superconductivity in LaFeAsO introduced the ferropnictides as a major new class of superconducting compounds with critical temperatures second only to cuprates. The presence of magnetic iron makes ferropnictides radically different from cuprates. Antiferromagnetism of the parent compounds strongly suggests that superconductivity and magnetism are closely related. However, the character of magnetic interactions and spin fluctuations in ferropnictides, in spite of vigorous efforts, has until now resisted understanding within any conventional model of magnetism. Here we show that the most puzzling features can be naturally reconciled within a rather simple effective spin model with biquadratic interactions, which is consistent with electronic structure calculations. By going beyond the Heisenberg model, this description explains numerous experimentally observed properties, including the peculiarities of the spin wave spectrum, thin domain walls, crossover from first to second order phase transition under doping in some compounds, and offers new insight in the occurrence of the nematic phase above the antiferromagnetic phase transition.

I. INTRODUCTION

The recent discovery of superconductivity in ferropnictides has ended the hegemony of cuprates and ushered in the new "iron era" in the studies of high-temperature superconductivity [1–3]. All parent ferropnictide compounds, unlike cuprates, are metallic and contain iron as the indispensable element. The occurrence of antiferromagnetism in the parent compounds of both cuprates and ferropnictides suggests that magnetism and superconductivity may be interrelated, and that the pairing mechanisms involve spin fluctuations in both cuprates and ferropnictides. However, magnetism in ferropnictides demonstrates a number of unique and puzzling properties, which are inconsistent with any conventional model. Understanding the character of magnetic interactions and spin fluctuations in ferropnictides is therefore of paramount importance for the problem of high-temperature superconductivity. In particular, a reasonable effective spin Hamiltonian supported by experimental measurements and theoretical calculations is highly desirable. Until now, such spin Hamiltonian has not been found. The purpose of this article is to solve this problem.

The antiferromagnetic (AFM) stripe ground state may be obtained in the Heisenberg model with appropriately chosen exchange parameters, such as the J_1-J_2 model with $J_2 > J_1/2$, which has been extensively studied in the context of frustrated magnetism [4]. However, this model neglects the large anisotropy of the nearest-neighbor exchange constant, which is firmly established both from first-principles calculations [5] and by neutron scattering measurements [2, 6, 7]. The three-dimensional character of magnetic interactions is also important [8]. Without these features, the Heisenberg model can not reproduce the qualitative features of the spin-wave spectrum. It is common to introduce the anisotropy of the exchange parameters explicitly; in particular, J_1 is split into J_{1a}

and J_{1b} for the pairs with antiparallel and parallel spins, respectively. Theoretically these parameters can be calculated using the linear response (LR) technique. The anisotropy of J_1 strongly depends on the local moment μ; J_{1b} (between parallel neighboring spins) can even change sign at large values of μ [9, 10]. Such strong dependence of the exchange parameters on the local moment clearly rules out the traditional Heisenberg model description for ferropnictides. Moreover, the anisotropy of exchange parameters breaks the symmetry of the spin Hamiltonian, which thereby becomes unsuitable beyond the spin-wave regime. In particular, magnetic phase transitions can not be described with such anisotropic Hamiltonian.

Another problem of the Heisenberg model is that it fails to describe the energies of noncollinear structures connecting the degenerate AFM domains. Specifically, in this model with interaction of any range the AFM domains with ordering vectors $(\pi, 0)$ and $(0, \pi)$ are connected by a continuous degenerate set of noncollinear states (at least at the mean-field level). In clear contradiction with this model, band structure calculations reveal the presence of a rather high energy barrier [9, 11] between $(\pi, 0)$ and $(0, \pi)$ states. In addition, it is difficult to reconcile the Heisenberg model with the fact that the domain walls between different AFM domains (both twin and antiphase) are very thin [12].

Failure of the Heisenberg model in ferropnictides led to the belief that the spin Hamiltonian approach has to be abandoned altogether in favor of a model that explicitly takes into account fermionic degrees of freedom. Strong anisotropy of the magnetic interaction in the stripe phase was argued to be linked with orbital ordering [13]. In the model with a non-interacting fermion sector added to the local moment subsystem, the double exchange is anisotropic in the stripe phase [14]. Although this model may be able to reproduce the spin wave spectrum, it contradicts transport measurements showing a rather moderate in-plane anisotropy of the resistivity, whose sign is opposite to that expected in the double exchange picture

[15]. In addition, it is not well suited for the studies of magnetic thermodynamics.

Thus, the Heisenberg model of any range clearly fails to describe the magnetism of ferropnictides. It is therefore natural to request a more refined theory which would (1) preserve the symmetry of the lattice, (2) generate the correct spin wave spectrum and anisotropic linear response properties in the stripe phase, (3) eliminate the spurious continuous ground state degeneracy, (4) be suitable for the studies of magnetic thermodynamics at finite temperatures, and (5) be consistent with electronic structure calculations. It is also desirable for the model to be capable of reproducing subtle features of magnetic thermodynamics observed in ferropnictides, including the occurrence of both first- and second- order phase transitions and the possibility of the nematic symmetry breaking. In this article we show that *all* these requirements can be met by including non-Heisenberg interaction in the effective spin Hamiltonian. The resulting effective Hamiltonian is found to explain numerous experimentally observed magnetic properties.

II. RESULTS

In the following, we justify the choice of the spin Hamiltonian, present an alternative interpretation of neutron scattering experiments, and then describe the magnetic thermodynamics in ferropnictides using the mean-field approximation and classical Monte Carlo simulations.

Model spin Hamiltonian

Our treatment is based on the following effective classical spin Hamiltonian:

$$H = \sum_{i<j} \left[J_{ij}\mathbf{S}_i\mathbf{S}_j - \tilde{K}_{ij} \left(\mathbf{S}_i\mathbf{S}_j \right)^2 \right] \tag{1}$$

The summation in (1) is taken over distinct pairs of lattice sites. The first term is the conventional (isotropic) exchange interaction, and the second term is the pairwise biquadratic interaction, which is the simplest and most natural form of non-Heisenberg coupling. We found that a consistent description of magnetism in ferropnictides is obtained using the J_1-K-J_2-J_c model, which includes the nearest and next-nearest in-plane exchange parameters J_1 and J_2, the interplane exchange parameter J_c, and the nearest-neighbor (in-plane) biquadratic coupling $K = \tilde{K}S^2$.

Note that a weak effective biquadratic interaction appears in the J_1-J_2 model through the "order-from-disorder" mechanism [4], and for pnictides it has been included in Ref. [16] assuming a very small interlayer coupling. Here we argue that a fairly strong biquadratic interaction is already present in the microscopic spin Hamiltonian in ferropnictides. Although magnetostructural coupling can also effectively induce non-Heisenberg

magnetic interactions, direct calculations [17] show that this distortion in the AFM phase has almost no effect on magnetic interactions.

The presence of non-Heisenberg terms in the Hamiltonian radically changes the interpretation of the LR exchange parameters J_{ij}^{LR}, which are defined as second derivatives of the total energy with respect to spin rotations. Rotating the spins at sites i and j in the opposite directions by an angle $\theta/2$, we find

$$J_{ij}^{\mathrm{LR}} \equiv -(\mathbf{S}_i\mathbf{S}_j)^{-1}\frac{\partial^2 H}{\partial\theta^2} = J_{ij} - 2\tilde{K}_{ij}S^2\mathbf{e}_i\mathbf{e}_j, \tag{2}$$

where $\mathbf{e}_i = \mathbf{S}_i/S$. The contribution of the biquadratic term depends on whether the spins in the given pair are parallel or antiparallel. For the stripe ground state, we find $J_{1a} = J_1 + 2\tilde{K}S^2$ and $J_{1b} = J_1 - 2\tilde{K}S^2$. Thus, the anisotropy of the nearest-neighbor LR exchange parameter in the stripe phase is captured by the biquadratic term in Hamiltonian (1).

Spin wave spectrum

The spin wave spectrum of $CaFe_2As_2$ was measured using inelastic neutron scattering in Refs. [6, 7] and fitted to the anisotropic J_1-J_2-J_c Heisenberg model. Here we reinterpret this fitting in terms of our *isotropic* J_1-K-J_2-J_c model, which produces an *identical* spin wave spectrum. The fitted value of K is strongly affected by the inclusion of the zone-edge magnons [7]. Table 1 shows the reinterpreted parameters of this fitting.

SJ_1	SK	SJ_2	SJ_c	J_sS^2	J_2/J_1	J_c/J_1	K/J_s	T_N, K	Order
22	14	19	5.3	35	0.86	0.24	0.16	90	I

TABLE I: Parameters of the model (in meV) fitted to spin wave spectrum [7]. Here $K = (J_{1a} - J_{1b})/4$, and $J_s = 4J_2 + 2J_c$. The parameter J_s and T_N are found assuming $S = 0.4$.

Fig. 1 illustrates the effect of K on the spin wave spectrum described by the following dispersion relations:

$$E(\mathbf{q}) = \sqrt{A_{\mathbf{q}}^2 - B_{\mathbf{q}}^2}, \tag{3}$$

where

$$A_{\mathbf{q}} = 2S[(J_1 - 2K)\cos(\pi k) + 4K + J_c + 2J_2] \tag{4}$$
$$B_{\mathbf{q}} = 2S[(J_1 + 2K)\cos(\pi h) + 2J_2\cos(\pi h)\cos(\pi k) + J_c\cos(\pi l)],$$

where $\mathbf{q}$ is the reduced wave vector (hkl). Starting from the values taken from Ref. [7] (Table 1), the evolution of the spectrum as K is decreased to zero is shown. As noted in Ref. [7], the absence of a minimum at the zone edge along the [010] direction signals a sign inversion of the parameter J_{1b}. Using spin Hamiltonian (1), this feature is immediately reinterpreted as a signature of a large value of biquadratic coupling $K > J_1/2$.
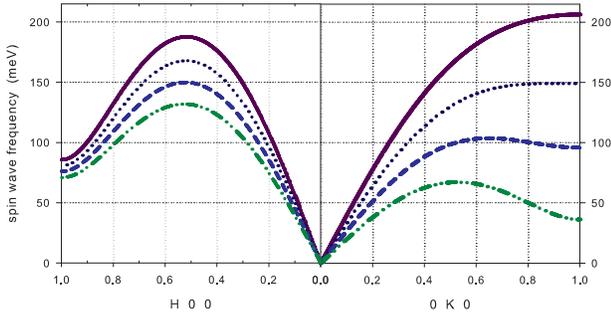
FIG. 1: Effect of the biquadratic coupling on the spin wave spectrum. The top curves correspond to the model parameters taken from Table 1. To obtain the other curves, from top to bottom, the ratio K/J_1 was reduced to 0.4, 0.2, and 0.

Mean-field phase diagram

In the presence of biquadratic interaction the single-site problem in MFA contains dipole and quadrupole effective fields with self-consistency required for both the magnetization $m_i = \langle \mathbf{e}_i \rangle$ and quadrupole order parameter $m_{ij} = \langle \mathbf{e}_i \mathbf{e}_j \rangle - \delta_{ij}/3$. Thus, apart from an AFM (stripe) phase with nonzero m_i, an anisotropic quadrupolar phase may appear with $m_i = 0$ but $m_{ij} \neq 0$ [18].

The MFA phase diagram is shown in the inset of Fig. 2. The only relevant phase up to $K/J_1 = 3$ is the AFM (stripe) phase. The most important feature for our purposes is the tricritical point at $K_t = 5J_s/24$, where $J_s = 4J_2 + 2J_c$. At $K = K_t$ the phase transition to the paramagnetic phase changes from second order (at lower K) to first order. At $K < K_t$ the transition temperature does not depend on K in MFA, while at $K > K_t$ there is a gradual crossover to a linear dependence. The tricritical point falls well within he range of realistic parameters for ferropnictides, and it is further significantly reduced by fluctuations (see below). Thus, magnetic Hamiltonian (1) can yield a first-order transition in ferropnictides without introducing any magnetostructural coupling (as it was done in Refs. [19]). This is a rather general feature of spin Hamiltonians with biquadratic coupling [18, 20].

At $K \approx J_s$ there is a triple point where the quadrupolar phase appears between the AFM and the paramagnetic phases. The quadrupolar phase is always separated from the paramagnetic phase by a first-order transition, but the AFM-to-quadrupolar transition changes from first to second order at a slightly higher K. The triple point occurs beyond the reasonable range of K for ferropnictides.

Monte Carlo simulations

The main results are presented in Fig. 2. We considered a few values of the J_2/J_1 ratio from 0.6 to 1.25 at fixed J_c/J_1=0.2, and a few values of J_c/J_1 at $J_2/J_1 = 0.6$. Note that $J_2/J_1 = 0.5$ is the stability limit

of the stripe phase at $T = 0$, and one can expect particularly strong fluctuations in the vicinity of this point. The fluctuations are also enhanced at small J_c/J_1, where two-dimensional behavior sets in.

As expected, the transition temperature is significantly reduced compared to MFA, and this reduction increases as J_2/J_1 approaches 0.5 and as J_c/J_1 decreases. Interestingly, the ratio K_t/J_s demonstrates a similar trend. The critical point for the parameters corresponding to $CaFe_2As_2$ is estimated at 90 K, which, considering the simplicity of the model, is in reasonable agreement with the experimental range of 140-170 K for 122 compounds. Further, this transition is of first order for these parameters, in agreement with experiment.
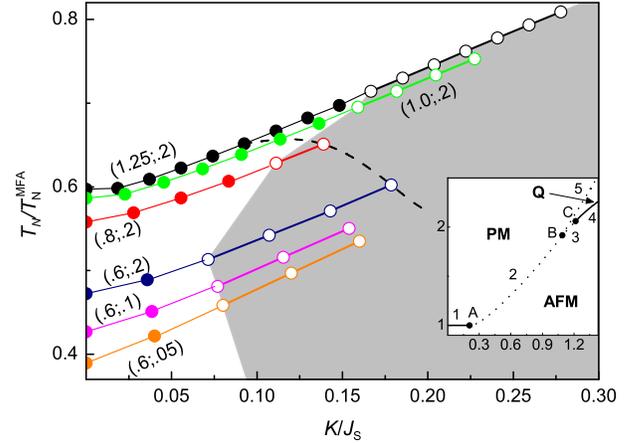

FIG. 2: Transition temperature and order of phase transition as a function of biquadratic interaction K obtained by Monte Carlo simulations. Temperature is measured in units of $T_N^{\mathrm{MFA}} = J_s/3$, which is the second-order T_N in MFA. Each line is labeled by a set of two parameters $(J_2/J_1; J_c/J_1)$. The region of first-order transitions (empty symbols) is schematically highlighted by shading and thicker lines. The dashed line shows the point of inversion of J_{1b}. The inset shows the mean-field phase diagram in a larger area of the same parameters. Solid lines 1 and 4 (dashed lines 2, 3 and 5) denote second-order (first-order) first transition. A and C are tricritical points; B is the triple point. Q denotes the quadrupolar phase.

Experimentally, a second-order AFM phase transition in ferropnictides is typically preceded by an orthorhombic structural transition. Between these transitions the so-called nematic phase occurs [3]. Theoretically, the nematic phase is known to occur at $J_c = 0$ [4] and was predicted to occur at $J_c \ll J_1$ as well [16]. It is not clear whether this phase can survive in the presence of substantial interplane and biquadratic interactions. It is rather difficult to establish the separation of the nematic and AFM phase transitions in Monte Carlo simulations, because the AFM correlation length becomes very large whenever this separation becomes large, and therefore a spurious "quasi-long-range-order" is generated by finite-size effects [21]. However, in a certain parameter range we have observed a clear signature of the nematic phase

in the finite-size behavior of the fourth-order cumulants of the nematic and AFM order parameters (their definitions are given in the *Methods* section). Fig. 3a shows the separation between the nematic and AFM phase transitions determined from the crossing points of the fourth-order cumulants for these order parameters calculated for different D (an example is shown in Fig. 3b). The separation determined in this way appears to increase at larger J_2/J_1, smaller K, and smaller J_c. It never occurs in the range of parameters where the phase transition is of the first order.
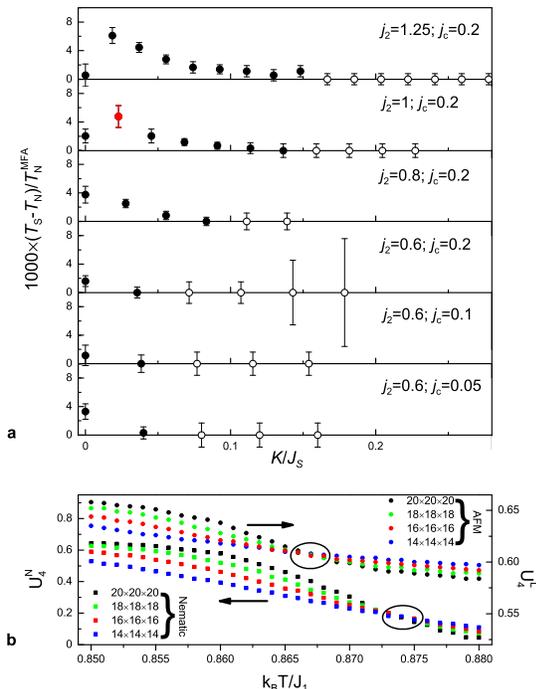

FIG. 3: (**a**) Relative separation of the nematic (T_s) and AFM (T_N) transition temperatures as a function of the biquadratic interaction parameter K for different values of $j_2 = J_2/J_1$ and $j_c = J_c/J_1$. Open (filled) symbols correspond to the first-order (second-order) phase transition. (**b**) Example of the separation of T_s and T_N in the finite-size scaling behavior of the respective fourth-order cumulants U_4^N and U_4^L; the parameters are for the point shown in red in panel **a**.

III. DISCUSSION

Since the K/J ratios are proportional to S^2, the AFM phase transition can change from first to second order if S is reduced. Such behavior was indeed observed under electron doping which reduces the local moments. Indeed, while the phase transition in updoped 122 compounds ($\mu \sim 0.8 - 0.9\mu_B$) appears to be first-order (most clearly in CaFe$_2$As$_2$ [22]), it changes to second order under electron doping [23, 24]. While the decrease of amplitude of the local moments in doped systems has not been measured, the critical temperature of magnetic phase

transition and the order parameter are clearly decreased with doping. The band structure studies further support this trend. The experimental situation with the local moment and order of the phase transition in LaFeAsO and other 1111 compounds is not yet fully resolved, but recent measurements suggest that they may be closer to 122 compounds than previously thought [25].

In view of the close proximity of the nematic and AFM phase transitions and the corresponding limitations of the finite-size scaling procedure, the signature of the separation of these transitions, while statistically robust, can not be viewed as the final proof. Still, it is remarkable that the separation appears to survive in an essentially three-dimensional case. In addition, contrary to Ref. 16, the biquadratic interaction is present on the level of microscopic Hamiltonian and is not small. Curiously, Fig. 3 suggests that at certain conditions the separation can go through a maximum as a function of K. The origin of this behavior remains to be understood.

Comparison of the effective spin Hamiltonian fitted to experiment (Table 1) with the results of first-principles calculations leads to an interesting observation. The experimental exchange parameters in Table 1 agree quite well with LR calculations [9, 10], except that the calculated value of K (which can be deduced either from the anisotropy of J_1 or from the height of the barrier between the two stripe states) reaches its experimental magnitude only for larger values of the local moment of order 1.4–1.8 μ_B. First-principles analysis of the dynamic susceptibility [17] also shows good agreement with experimental spin wave spectrum if the local moment is of that order. On the other hand, scaling of the spin moment up by a factor of two would also scale up the predicted T_N (Table 1) by a factor of two and bring it in almost quantitative agreement with experiment. This observation seems to support the notion that the (mean-field) local moments in ferropnictides are roughly twice their observed values, which may be screened by dynamical fluctuations.

We have shown that a consistent model of magnetism in ferropnictides is obtained by introducing biquadratic interaction in the model spin Hamiltonian. This model satisfies all reasonable requirements, reproduces many experimental observations, and is supported by electronic structure calculations. As a word of caution, the success of the localized model spin Hamiltonian should not be taken to rule out itinerant effects. On the contrary, the effective spin model should be viewed as an appropriate mapping of the complicated itinerant interactions, which include complicated rearrangements of the Fermi surface and density matrices induced by magnetic ordering. This interpretation is supported by the fact that a large biquadratic term appears at relatively low values of the local moment. We find it appropriate to speculate that strong non-Heisenberg coupling in the effective spin model, being a consequence of strong coupling between the itinerant electrons and spin fluctuations, explicitly suggests spin fluctuations as a possible pairing mechanism in ferropnictides.

4

IV. METHODS

We have studied tetragonal lattices $D \times D \times D$ with periodic boundary conditions, where $D = 14$, 16, 18, and 20. Looping over the lattice sites, a new random spin direction for the given spin is tried and accepted or rejected using the Metropolis prescription. The averages are accumulated during a sufficiently long measurement run after an initial equilibration run. The lengths of these runs were adjusted in order to obtain sufficient accuracy. The AFM order parameter L is defined as $L^2 = L_x^2 + L_y^2$, where L_x and L_y are the staggered order parameters with the x and y staggering direction, respectively. The nematic order parameter is defined as $N = \left| \frac{1}{2} \sum_i \sum_{nn} \eta_{ij} \mathbf{S}_i \cdot \mathbf{S}_j \right|$, where the sum is over the four in-plane nearest neighbors, and η_{ij} is equal to ± 1 with opposite signs taken for the two perpendicular directions. The order of the phase transition was determined by analyzing the behavior of the fourth-order energy cumulant [26]. If this cumulant converges toward the value $2/3$ for all temperatures with increasing D, the transition is of second order. On the other hand, if the energy cumulant develops a minimum at some temperature, which becomes sharper with increasing D, the transition is of first order [26]. If the transition was found to be of second order, the critical temperatures for the AFM and nematic transitions were determined from the finite-size scaling behavior of the fourth-order cumulant of the respective order parameter [27]. For first order transitions, the transition temperatures for AFM and nematic phase transition were found from the peaks of the corresponding susceptibilities.

[1] I. I. Mazin, Nature **464**, 183 (2010).

[2] J. W. Lynn and P. Dai, Physica C **469**, 469 (2009).

[3] D. C. Johnston, Adv. Phys. **59**, 803 (2010).

[4] P. Chandra, P. Coleman, and A. I. Larkin. Phys. Rev. Lett. **64**, 88 (1990).

[5] Z. P. Yin, S. Lebègue, M. J. Han, B. Neal, S. Y. Savrasov, W. E. Pickett, Phys. Rev. Lett. **101**, 047001 (2008).

[6] S. O. Diallo, V. P. Antropov, T. G. Perring, C. Broholm, J. J. Pulikkotil, N. Ni, S. L. Bud'ko, P. C. Canfield, A. Kreyssig, A. I. Goldman, and R. J. McQueeney, Phys. Rev. Lett. **102**, 187206 (2009).

[7] J. Zhao, D. T. Adroja, D.-X. Yao, R. Bewley, S. Li, X. F. Wang, G. Wu, X. H. Chen, J. Hu, P. Dai, Nature Phys. **5**, 555 (2009).

[8] R. J. McQueeney, S. O. Diallo, V. P. Antropov, G. Samolyuk, C. Broholm, N. Ni, S. Nandi, M. Yethiraj, J. L. Zarestky, J. J. Pulikkotil, A. Kreyssig, M. D. Lumsden, B. N. Harmon, P. C. Canfield, and A. I. Goldman, Phys. Rev. Lett. **101**, 227205 (2008).

[9] J. J. Pulikkotil, L. Ke, M. van Schilfgaarde, T. Kotani, and V. P. Antropov, Supercond. Sci. Technol. **23**, 054012 (2010).

[10] M. J. Han, Q. Yin, W. E. Pickett, and S. Y. Savrasov, Phys. Rev. Lett. **102**, 107003 (2009).

[11] A. N. Yaresko, G.-Q. Lin, V. N. Antonov, and O. K. Andersen, Phys. Rev. B **79**, 144421 (2009).

[12] T.-M. Chuang, M. P. Allan, J. Lee, Y. Xie, Ni Ni, S. L. Budko, G. S. Boebinger, P. C. Canfield, and J. C. Davis, Science **327**, 181 (2010); G. Li, X. He, A. Li, S. H. Pan, J. Zhang, R. Jin, A. S. Sefat, M. A. McGuire, D. G. Mandrus, B. C. Sales, and E. W. Plummer, arXiv:1006.5907.

[13] F. Krüger, S. Kumar, J. Zaanen and J. van den Brink. Phys. Rev. B **79**, 054504 (2009); C.-C. Lee, W.-G. Yin, and W. Ku, Phys. Rev. Lett. **103**, 267001 (2009); C.-C. Chen, J. Maciejko, A. P. Sorini, B. Moritz, R. R. P. Singh, and T. P. Devereaux. Phys. Rev. B **82**, 100504 (2010).

[14] W. Lv, F. Krüger, and P. Philips, Phys. Rev. B **82**, 045125 (2010); C. Lee, W. Lin and W. Ku, Phys. Rev. Lett. **105**, 107004 (2010).

[15] M. A. Tanatar, E. C. Bloomberg, A. Kreyssig, M. G. Kim, N. Ni, A. Thaler, S. L. Bud'ko, P. C. Canfield, A. I. Goldman, I. I. Mazin, and R. Prozorov, Phys. Rev. B **81**, 184508 (2010); J.-H. Chu, J. G. Analytis, K. de Greve, P. L. McMahon, Z. Islam, Y. Yamamoto, and I. R. Fisher, Science **329**, 824 (2010).

[16] C. Fang, H. Yao, W.-F. Tsai, J. Hu, S. A. Kivelson, Phys. Rev. B **77**, 224509 (2008).

[17] L. Ke, M. van Schilfgaarde, J. J. Pulikkotil, T. Kotani, and V. P. Antropov, arXiv:1004.2934.

[18] V. M. Matveev and E. L. Nagaev, Sov. Phys. – Solid State **14**, 408 (1972).

[19] V. Barzykin and L. P. Gor'kov. Phys. Rev. B **79**, 134510 (2009); R. M. Fernandes, L. H. VanBebber, S. Bhattacharya, P. Chandra, V. Keppens, D. Mandrus, M. A. McGuire, B. C. Sales, A. S. Sefat, and J. Schmalian, Phys. Rev. Lett. **105**, 157003 (2010).

[20] E. L. Nagaev, Sov. Phys. Uspekhi **25**, 31 (1982).

[21] O. Kapikranian, B. Berche, and Yu. Holovatch, J. Phys. A: Math. Theor. **40**, 3741 (2007).

[22] N. Ni, S. Nandi, A. Kreyssig, A. I. Goldman, E. D. Mun, S. L. Bud'ko, and P. C. Canfield, Phys. Rev. B **78**, 014523 (2008).

[23] N. Ni, A. Thaler, A. Kracher, J. Q. Yan, S. L. Bud'ko, and P. C. Canfield, Phys. Rev. B **80**, 024511 (2009); E. D. Mun, S. L. Bud'ko, N. Ni, A. N. Thaler, and P. C. Canfield, Phys. Rev. B **80**, 054517 (2009).

[24] R. M. Fernandes, D. K. Pratt, W. Tian, J. Zarestky, A. Kreyssig, S. Nandi, M. G. Kim, A. Thaler, N. Ni, P. C. Canfield, R. J. McQueeney, J. Schmalian, and A..I.

Goldman, Phys. Rev. B **81**, 140501(R) (2010).

[25] N. Qureshi, Y. Drees, J. Werner, S. Wurmehl, C. Hess, R. Klingeler, B. Buechner, M. T. Fernandez-Diaz, and M. Braden, arXiv:1002.4326; H.-F. Li , W. Tian, J.-Q. Yan, J. L. Zarestky, R. W. McCallum, T. A. Lograsso, and D. Vaknin, arXiv:1007.2197.

[26] M. S. S. Challa, D. P. Landau, and K. Binder, Phys. Rev. B **34**, 1841 (1986).

[27] K. Binder, Z. Phys. B **43**, 119 (1981).